ELSEVIER

Agricultural and Forest Meteorology 108 (2001) 1–14

AGRICULTURAL AND FOREST METEOROLOGY

www.elsevier.com/locate/agrformet

Estimation of leaf area index in open-canopy ponderosa pine forests at different successional stages and management regimes in Oregon

B.E. Law [a,*], S. Van Tuyl [a], A. Cescatti [b], D.D. Baldocchi [c]

[a] *Department of Forest Science, Richardson Hall, Oregon State University, Corvallis, OR 97331, USA*
[b] *Centro di Ecologia Alpina, I-38040 Viote del Monte Bondone (TN), Italy*
[c] *Department of Environmental Science, Policy and Management, University of California, Berkeley, CA 94720, USA*

Received 21 November 2000; received in revised form 23 January 2001; accepted 26 January 2001

Abstract

Leaf area and its spatial distribution are key parameters in describing canopy characteristics. They determine radiation regimes and influence mass and energy exchange with the atmosphere. The evaluation of leaf area in conifer stands is particularly challenging due to their open nature and clumping on the needle, shoot and tree scale. The overall objective of our study was to characterize leaf area index (LAI) (L_h, m^2 half-surface area foliage m^{-2} ground) in the vicinity of our old-growth and 14-year-old ponderosa pine (*Pinus ponderosa*, var. Laws) eddy covariance flux sites, with future plans to scale from the flux sites to the pine region using ecosystem models and remote sensing. From the combination of optical and canopy geometry measurements, sapwood and litter-fall measurements, and one- and three-dimensional (3-D) models, we evaluated the variation in estimates of L_h in a mixed-age stand at the old-growth flux site. We also compared sapwood area estimates from a local allometric equation with LAI-2000 estimates that have been corrected for clumping and the interception of light by stems and branches (L_{hc}, m^2 half-surface area m^{-2} ground) across a range of age classes and stand densities of ponderosa pine forests along a 15 km swath in Central Oregon that encompassed the flux sites. In the old-growth stand, the litter-fall and sapwood estimates tended to be higher than the optical and 3-D radiative transfer model estimates. Across the 15 km east–west gradient from the crest of the Cascade Mountains, L_{hc} was typically lower than the sapwood estimates (L_{hsw}; slope 0.38). The L_{hc} data, as well as aboveground production estimates for the 17 pine plots will be useful for scaling flux measurements to the region using ecosystem models that have been validated with these data.

Keywords: Leaf area; Canopy architecture; Radiative transfer; Carbon exchange; Energy exchange; *Pinus ponderosa*; Soil-vegetation-atmosphere transfer (SVAT) modeling

1. Introduction

The US Carbon Cycle Plan (1995) calls for an accurate accounting of terrestrial carbon (C) budgets, stressing that an observational network of flux measurements and predictive models of interannual to decadal carbon cycle dynamics should be important components for understanding processes that control the temporal trends and spatial distribution of CO_2 sources and sinks. Several studies have attempted to estimate C budgets over large regions (e.g. VEMAP Members, 1995; Houghton et al., 1998). A numerical

* Corresponding author. Tel.: +1-541-737-6111; fax: +1-541-737-1393.
E-mail address: lawb@fsl.orst.edu (B.E. Law).

0168-1923/01/$ – see front matter
PII: S0168-1923(01)00226-X

simulation approach, combined with remote sensing and a network of validation sites may be the best way to produce a reasonable regional carbon budget analysis, but such efforts have been stymied by lack of a robust observational framework for multi-scaled model evaluation.

The controls on ecosystem processes are being substantiated by observations of net carbon exchange of CO_2 (NEE) and H_2O from tower flux measurement sites in various vegetation types across a range of climatic conditions (Oechel et al., 1998; Hollinger et al., 1999; Law et al., 2000a,b). These sites serve as important validation sites for ecosystem models that are being applied spatially to estimate NEE. Leaf area is an important characteristic because of the role of foliage in intercepting photons and serving as a source or sink for the transfer of energy, carbon, and water vapor exchange between forested ecosystems and the atmosphere through stomatal conductance (photosynthesis, respiration, and transpiration). The ecosystem models require either field validation of simulated leaf area index (LAI), or remotely sensed estimates of LAI to initiate them. Previous work has shown that model estimates of NEE can be low by at least 15–20% by ignoring the impacts of clumping on light transfer, the computation of sunlit and shaded leaves, and photosynthesis and stomatal conductance (Baldocchi and Harley, 1995). This stresses the need to account for clumping if optical approaches are used to estimate LAI (Chen, 1996).

Some studies have compared direct and indirect methods of estimating LAI (e.g. Fassnacht et al., 1994). Gower et al. (1999) synthesized data from independent studies across forest types and showed that indirect estimates of LAI plateau around 5–6, while direct estimates reach 9. They proposed that direct measurement of LAI is the only reliable approach for dense canopies with LAI > 6. The caveat is that the most desirable approach to direct measurements is to develop site-specific allometric equations, which requires destructive harvesting. This may not be feasible in many locations, and it is very time-consuming compared with optical estimates. Foliage allometric equations from other locations should be used with caution because they are influenced by tree size, species, and edaphic conditions. For low leaf area forests, optical estimates that have been corrected for clumping may be sufficient.

We have been making biological and flux measurements in ponderosa pine (*Pinus ponderosa*, var. Laws) in the semi-arid region of Oregon, where canopies are more open and LAI values are relatively low. We have also participated in model-testing exercises, which often required accurate estimates of LAI (Law et al., 2000a, b, 2001). In this paper, we compare methods for estimating LAI (L_h, m^2 half-surface area of foliage per m^2 ground) in the field with a suite of measurements at two pine flux sites, using optical (LAI-2000 measurements corrected for clumping and Decagon ceptometer) and more traditional approaches, such as litter-fall, and sapwood area estimates based on the pipe model theory (Waring et al., 1982). In addition, we determined the range of L_h values for ponderosa pine plots along a 15 km swath using both LAI-2000 and sapwood basal area approaches (e.g. Turner et al., 1999) in preparation for extending the analysis more broadly using remote sensing. These plots allow us to evaluate LAI estimates over a range of conditions within a particular forest type, including stand density, tree heights, and site quality.

2. Methods

2.1. Site description

We conducted the study on the east side of the Cascade Mountains in Central Oregon, where there is a strong climatic gradient and a transition from Douglas-fir (*Pseudotsuga menziesii*) to the dry eastern extent of ponderosa pine. The climate of the ponderosa pine zone is semi-arid (annual precipitation ranges from ∼350 to 880 mm), with minimal summer precipitation. These forests typically have relatively discontinuous canopies with low leaf areas.

Measurements for the comparison of several methods of estimating LAI were made during the summer of 1997 in an old-growth ponderosa pine forest located in a Research Natural Area in the Metolius River basin (44°30′N, 121°37′W, elevation 940 m, 1% slope) east of the Cascade Mountains in Oregon. Sapwood and optical measurements were repeated at this plot in 1999, and at 14 additional ponderosa pine plots along a 15 km east–west swath, including our 15-year-old pine flux site (Fig. 1).

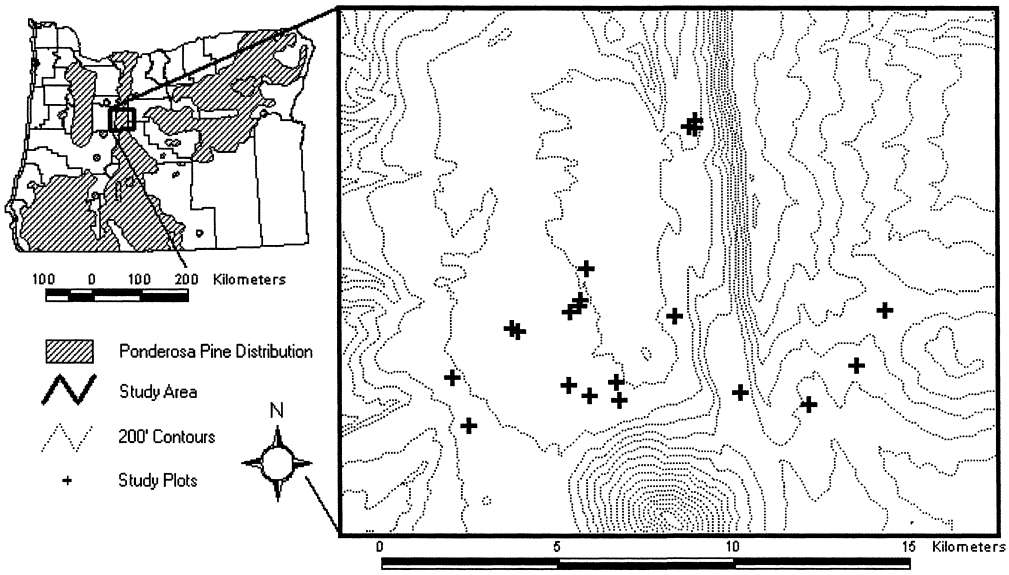

Fig. 1. Location of research plots in the Metolius area, Central Oregon.

Ponderosa pine needles are long (18–20 cm), three per fascicle, and clustered at the outer 20–50 cm of shoots. Each needle is not perfectly round, so it will affect the light interception and distribution (Oker-Blom and Kellomaki, 1982). In the study area, the trees carry 3–4 years of foliage. Older trees are free of branches on the lower half to two-thirds of the stems, with conical or almost flat-topped crowns. Our phenology data show that budswell was initiated at the end of May, budbreak occurred mid-June, and needle elongation was completed by the last week of August at the young and old-growth flux sites in 1999, a La Niña year when late winter snows delayed phonological development by about 2 weeks.

The old-growth site consists of a mosaic of mixed-age stands (45% of the area), pure old-growth (27%), and dense patches of young trees (∼45-year-old, 25% of the area). The understory is sparse with patches of bitterbrush (*Purshia tridentata*) and bracken fern (*Pteridium aquilinum*), and ground cover of strawberry (*Fragaria vesca*). The 14-year-old pine flux site was previously old-growth that had been clearcut, and then seeded in by natural regeneration. Such stands typically have a large component of understory shrubs. Understory at the young flux site is primarily manzanita (*Arctostaphylos patula*) and bitterbrush. The remaining pine sites where we measured canopy geometry and LAI range from even-aged mature stands (thinned and unthinned), to young, naturally regenerating stands, and old-growth stands. Table 1 shows general characteristics for all plots.

2.2. Optical measurements

Our plot design for optical measurements was a systematic grid over a 100 m × 100 m plot. The tree dimension measurements were made on a cluster of five 10 m radius subplots within the plot. This design was chosen because it was more efficient for linking optical and tree dimension measurements to a radiative transfer model (Law et al., 2001). The plot size ensured fairly homogeneous conditions appropriate for remote sensing validation efforts (e.g. pixel size 30 m).

In 1997, we established a 100 m × 100 m plot in a mixed-age age ponderosa pine stand (Plot 1) at our old-growth flux site, where we used multiple measurement methods for estimating LAI. Optical measurements were made with a LAI-2000 (LICOR, Lincoln, NE) in September under diffuse light conditions (twilight) at 5 m grid points on a systematic grid (121 sample locations per plot). The same kinds of optical measurements were made at 10 m intervals

Table 1
Characteristics of ponderosa pine stands (plot numbers are not consecutive because remaining plots were dominated by other species)[a]

Plot	Longitude	Latitude	Stand density (no. of trees/ha)	Tally tree density (<5 cm DBH) (no. of trees/ha)	Age	Site index (m)	Mean DBH (cm)	Mean height (m)	Mean height to base of crown (m)	Species composition	Treatment
1	−121.626	44.499	694, 59	82	52 (7.7), 250	21	12.3 (5.05), 68.6 (3.10)	9.6 (3.44), 33.9 (1.32)	4.48, 9.51 (0.08, 0.47)	Pipo	Natural, two layer canopy
2	−121.623	44.500	84	0	250	21	54.9 (2.51)	33.5 (1.26)	12.09 (0.48)	Pipo	Natural, single layer canopy
3	−121.623	44.498	1286	0	56 (9.5)	18	15.3 (0.99)	12.1 (0.52)	6.78 (0.20)	Pipo	Natural, single layer canopy
4	−121.631	44.451	236, 64	1572	20, 160	31	9.0 (0.40), 71.5 (7.20)	5.1 (0.20), 36.0 (2.78)	1.71, 12.35 (0.07, 1.93)	Pipo	Natural, two layer canopy
5	−121.652	44.435	382	19	81 (12)	15	23.9 (1.37)	13.7 (0.76)	5.57 (0.32)	Pipo	Thinned, single layer canopy
6	−121.668	44.453	866	70	80	12	17.0 (0.75)	11.8 (0.42)	6.25 (0.19)	Pipo	Natural, single layer canopy Shallow water table
7	−121.665	44.454	509	76	97 (15)	18	23.5 (1.32)	17.6 (0.97)	6.25 (0.48)	Pipo, Laoc, Abgr	Natural, single layer canopy Shallow water table
8	−121.664	44.456	331	95	83 (5)	21	25.0 (2.05)	19.2 (1.50)	8.09 (0.94)	Laoc, Pipo, Abgr	Natural, single layer canopy Shallow water table
9	−121.687	44.448	210	19	52 (9)	21	23.1 (1.22)	13.3 (0.67)	5.53 (0.35)	Pipo	Heavily thinned, single layer canopy
10	−121.584	44.428	261	134	40	18	24.6 (1.05)	8.7 (0.37)	1.40 (0.10)	Pipo	Clear-cut, natural regeneration
11	−121.556	44.451	363	204	35 (12)	31	29.2 (0.82)	14.2 (0.39)	3.57 (0.18)	Pipo	Thinned, single layer canopy
15	−121.662	44.431	12, 22	554	64, 158	24	23.9 (1.94), 69.1 (5.56)	11 (1.02), 30.7 (1.48)	2.96, 7.52 (0.46, 0.73)	Pipo	Heavily thinned, two layer canopy
16	−121.669	44.434	458	140	60 (13)	21	22.8 (1.36)	15.2 (0.76)	6.85 (0.35)	Pipo, Laoc, Pico, Psme	Natural, single layer canopy Shallow water table
17	−121.662	44.464	528	210	55 (4)	18	19.0 (1.33)	12. 7 (0.83)	3.63 (0.30)	Pipo, Laoc, Pico, Psme	Natural, single layer canopy
18	−121.608	44.431	465	503	174 (40)	9	23.5 (2.65)	10.6 (1.14)	2.91 (0.31)	Pipo, Cade	Natural, two layer canopy
19	−121.651	44.430	312	490	63 (14)	18	13.1 (1.29)	12 (0.69)	4.77 (0.28)	Pipo	Thinned, single layer canopy
20	−121.567	44.438	344	949	14 (1)	24	10.4 (0.46)	4.3 (0.16)	0.77 (0.05)	Pipo	Clearcut, natural regeneration

[a] Species codes — Abgr: *Abies grandis*, Cade: *Calocedrus decurrens*, Laoc: *Larix occidentalis*, Pico: *Pinus contorta*, Pipo: *Pinus ponderosa*, Psme: *Pseudotsuga menziessii*.

in july 1999 at Plot 1. Plots of the same dimensions were also measured at a pure old-growth stand (Plot 2) and a dense young stand (45-year-old, Plot 3) at the old-growth flux site, 14-year-old flux site, and at 11 additional locations in the 15 km swath from the western extent of ponderosa pine on the east slope of the Cascade Mountains.

Prior to measurements, the two LAI-2000 sensors were synchronized and calibrated to one another in an open field large enough that trees around the perimeter were not blocking the sensor view. One sensor was left in the field to record incident light automatically. The sensor used for below-canopy transmittance was held at 2 m height and levelled from below. We did not use a view restrictor. For understory, measurements were made at the same grid points below the shrub cover, using a 90° view restrictor to ensure that the operator was not in view. Data were processed with software to match ambient and transmittance measurements in time (Comm.exe, A. Cescatti), and the LAI-2000 software (c2000.exe) was used to calculate effective leaf area (L_e) for each measurement point. Understory leaf area was calculated as the difference between total L_e and overstory L_e. The plot mean was obtained, then corrected by

$$L_{hc} = (1 - \alpha) L_e \times \frac{\gamma_E}{\Omega_E} \quad (1)$$

where L_{hc} is m^2 half-total surface area (HSA) of needles per m^2 ground corrected for clumping of needles within shoot, and at scales larger than shoot, and interception by wood, γ_E the needle-to-shoot area ratio for foliage clumping within shoot, Ω_E the element clumping index that quantifies the effect of foliage clumping at scales larger than the shoot, and α the woody-to-total area ratio ($\alpha = W/(L_e \times \gamma_E/\Omega_E)$). If shoots are randomly positioned in the canopy, then correction with Ω_E is not necessary. However, conifer canopies are highly organized at the shoot, branch, whirls, and crown level. This grouping results in a canopy gap fraction that is larger than that of a random canopy. There can be different gap size distributions for the same canopy gap fraction, thus the gap size distribution can be used to quantify the effects of canopy architecture on optical LAI measurements that are based on the gap fraction principle. Chen and Cihlar (1995) theory for calculating Ω_E addresses this issue. W is wood surface area index (half-total wood surface area m^{-2} ground, including branches (B) and stems (S)). This approach assumes that woody materials have a spatial distribution similar to foliage, and may result in a small error in the LAI estimates (Chen et al., 1997b). The theoretical basis of Eq. (1) is derived and discussed in detail in Chen (1996) and in Chen and Cihlar (1995).

To determine stem area for W, we used our measurements of diameter at breast height (DBH) and tree height that we made on the five 10 m radius subplots within each 10 000 m^2 plot. For each tree, we calculated half-surface area of a cylinder from the ground to DBH, the frustum of a cone for four segments of equal height, and a cone for the tree-top (sixth segment). We used an allometric equation from the literature for ponderosa pine to estimate branch biomass per m^2 ground (Gholz, 1982), and our site measurements of density of wood cores (10 cores per plot) to calculate branch volume per m^2 ground. This was converted to half-branch area from the mean branch radius in diameter classes, when necessary (e.g. 0–30 cm, >30 cm DBH for the mixed-age plot at the old-growth site).

We determined Ω_E from continuous measurements with a TRAC (3rd Wave Engineering, Ontario, Canada) along two 100 m transects within each plot. TRAC measures canopy gap size distribution and canopy gap fraction with a high frequency sampling technique. Transects were chosen based on the sun angle in relation to the plot, extreme high and low sun angles were avoided to reduce error in the measurements (e.g. difficulty distinguishing small gaps at solar zenith angles >60°). Transects were measured at a pace of 10 m every 30 s as suggested in the TRAC manual. Using TRAC software (TRAC.exe, J. Chen), a gap accumulation curve is produced, where the gap fraction is accumulated from the largest to the smallest gap, then a gap removal method is used to quantify gaps resulting from non-randomness of the canopy (Chen and Cihlar, 1995). The clumping effect, Ω_E, is then determined from the difference between measured gap fraction and gap fraction after removal of gaps resulting from non-randomness.

We also quantified Ω_E over a range of solar zenith angles from photosynthetically active radiation measurements 1.5 m above the forest floor with a quantum sensor (model LI-190S, LICOR, Lincoln, NE) mounted on an automated tram system that traversed 36 m horizontally at a rate of 1 cm s^{-1}, so that a

sample was taken every millimeter. The tram sensor traveled east and west over the northern portion of the 10 000 m^2 plot (day 189–205, 1996).

The needle-to-shoot area ratio (γ_E) was calculated from

$$\gamma_E = A_{tn}/4\bar{A}_p \quad (2)$$

where A_{tn} is total needle surface area on a shoot and $\bar{A}_p$ the mean of the projected shoot silhouette areas (Stenberg, 1996). We used γ_E values calculated in the previous study on ponderosa pine, and from the literature for the other species in the mixed-species stands (Law et al., 2001; Chen and Black, 1992; Gower and Norman, 1991). For mixed-species plots, we weighted γ_E for a species by the fraction of total number of trees per hectare. We determined A_{tn} in the previous study from leaf area meter measurements of projected area, corrected with a conversion factor (2.36) for ponderosa pine needle geometry, then divided by two to get HSA. Projected shoot silhouette areas were determined from photographs of shoots held at three projections and four angles, then processed in Adobe Photoshop (Adobe Systems, Inc., San Jose, CA, Version 5.0) and ImageTool (Version 2.0, University of Texas Health Science Center).

Plots 10 and 20 (14-year-old pine flux site) had significant amounts of understory present. We compared three methods for estimating understory L_h at Plot 20, the LAI-2000 grid point method that we used for all plots, LAI-2000 measurements under individual shrubs, and destructive harvest. We used the LAI-2000 with a 90° view restrictor, and made measurements in 4 cardinal directions under 5 shrubs of each species that covered the range of sizes present. The shrub dimensions were measured ($l \times w \times h$), and the shrubs were harvested for determination of leaf area per plant. The optical measurements of leaf area density were multiplied by the shrub volume/ground area to get L_h per shrub, which was then multiplied by percentage cover of each shrub size class to estimate shrub L_h for the plot. The harvest estimates of shrub L_h were also scaled to the plot by percentage cover in each size class.

At Plot 1 in 1997, we made concurrent measurements of ambient photosynthetically active radiation (PAR, Q_o) and canopy transmittance (Q_t) with Decagon Ceptometers (Decagon Devices, Pullman, Washington) at mid-day under clear skies following methods described by Law and Waring (1994). Ambient direct and diffuse PAR were recorded continuously at the top of the flux tower. Transmitted PAR measurements were made with a Ceptometer every 10 m on the 100 m × 100 m plot ($n = 121$). LAI was calculated from Ceptometer data and the equation (Campbell, 1991)

$$L_{ecep} = \frac{[f_b(1 - \cos\theta) - 1]\ln(Q_t/Q_o)}{A(1 - 0.47f_b)} \quad (3)$$

where A is 0.84 for leaf absorptivity (a) of 0.90 in the PAR band ($A = 0.283 + 0.785a - 0.159a^2$), f_b the fraction direct beam, and θ the solar zenith angle calculated from latitude (44.5°N), day, and hour of day (Rosenberg et al., 1983).

2.3. Tree dimensions

Tree dimension and location data were needed to drive the 3-D radiative transfer model for Plot 1, and stand density and sapwood area were required for the sapwood estimates of L_h at all plots. The cluster of five 10 m radius subplots at each plot was arranged with one subplot in the center, and one 30 m from each corner of the plot. We sampled all trees on the pure old-growth plot (Plot 2), because of the low density. For trees larger than 5 cm DBH (measured at 1.3 m from the ground), we measured DBH, total height, height to the base of live crown, and height and radius of the widest portion of the crown in two to four orthogonal directions using a laser technology (Impulse 200, Laser Technology, Englewood, CO). Locations of plot corners and subplot centers were measured with a global positioning system (PathFinder Pro, Trimble Navigation Limited, Sunnyvale, California), and differentially corrected with Portland, Oregon base station data. Tree locations in the subplots were mapped using a unit attached to the laser (MapStar, Pacific Survey, Inc.). Trees smaller than 5 cm DBH were tallied, except in young stands, where we measured dimensions on all trees on the subplots. We cored two trees per subplot for sapwood area estimates per tree.

2.4. Litter-fall and sapwood allometric estimates of leaf area

Direct measurement of leaf area by destructive harvest was not possible. Instead, we estimated L_h from

allometry based on harvests in nearby stands, and from litter-fall. The sapwood allometric estimates of L_h were based on the pipe-model theory (Waring et al., 1982). We estimated sapwood area (A, cm^2 sapwood) of trees on which we did not take cores by applying plot-specific regression equations in the form of

$$\log A_{sw} = a + b(\log \mathrm{DBH}), \quad (4)$$

where log is the $base_{10}$ logarithmic transformation. The equations were corrected for logarithmic bias using

$$\mathrm{CF} = \exp[\tfrac{1}{2}(2.303(\mathrm{MSE}^{1/2}))^2]$$

where CF is the correction factor that the dependent variable, A_{sw}, was multiplied by, and M.S.E. the $\log_{10}$ transformed regression mean square error (Sprugel, 1983). We pooled cores from a few plots where the initial number of cores was inadequate, once we determined that slopes and intercepts were not different and that stand density and age were similar (cores from Plots 5 and 19, and from 6, 7, 8 and 17). To estimate leaf area from sapwood area (m^2 HSA m^{-2} ground), we applied a linear regression developed from sapwood area at breast height (sapwood range < 100–$800\,cm^2$) in ponderosa pine near our site (O'Hara and Valappil, 1995):

$$L_{hsw} = (0.163 \times A_{swi} - 2.594) \times T \quad (5)$$

where A_{swi} is cm^2 sapwood area in the diameter class i, and T the number of trees per m^2 ground in the diameter class. For stands with two distinct diameter classes, we determined L_{hsw} for each class and then summed L_{hsw} for the plot.

We collected litter-fall from nine traps located within Plot 1 (each trap $0.13\,m^2$) periodically through the year (March 1996–1997). The litter was separated into foliage and woody litter, oven-dried at 75°C for 48 h, weighed and then summed for the year. L_{hlit} was calculated from specific leaf area of foliage litter (SLA $= 43.8\,cm^2$ half-surface area needles g^{-1}), biomass of foliage litter ($M_{lit} = 174\,g\,m^{-2}$ ground), fractional mass loss on abscission ($f_{abs} = 0.15$), and foliage turnover rate of 25% ($f_t = 0.25$)

$$L_{hlit} = \frac{M_{lit} \times (1 + f_{abs}) \times \mathrm{SLA}}{f_t} \quad (6)$$

2.5. Three-dimensional radiative transfer modeling

Spatially explicit LAI-2000 measurements were coupled with a 3-D canopy model, FOREST (Cescatti, 1997a), which reproduces stand geometry by accounting for position and crown shape of single trees on the plot. Full details of model development and formulae are provided in Cescatti (1997a). The canopy structure of each tree is described in the model with stratification into three asymmetric crown envelopes, that represent different densities of branch and leaf area. The input variables for canopy structure are total tree height, height to base of crown, height at the widest point of the crown, crown radii in four orthogonal directions, and shape coefficients of vertical crown profiles. The vertical distribution of leaf area within a crown, LAD, is modelled using a Beta or Weibull equation. The effect of the spatial pattern of leaf area is taken into account by simulating random, regular or clumped distributions. The probabilities of penetration of direct and diffuse radiation are modeled separately using a Markov model (Nilson, 1971). Diffuse radiation resulting from scattering is estimated on the basis of the adding method (Norman and Jarvis, 1975). Given the co-ordinates of the sampling points, the model generates a hemispherical view of the canopy as seen from the LAI-2000 (Cescatti, 1997b), and predicts canopy transmittance for the five rings of the LAI-2000 sensor. To avoid edge effect, only the LAI-2000 sampling points well within Plot 1 were used in the inversion. Only the values of canopy transmittance in the three intermediate rings (2, 3 and 4) were used. The inner LAI-2000 ring (1) was excluded because measurements by this ring are overly sensitive to the sensor position with respect to crown projections. The external ring (5) was excluded because measurements of canopy transmittance in this ring are biased by scattered radiation.

The indirect estimation of LAI was performed by changing the leaf area density in the crown layers iteratively to minimize the square error between the model prediction and the LAI-2000-measured transmittance according to the Quasi-Newton algorithm. The value of leaf area density minimizing the sum of square errors was used to calculate leaf area of each tree and the stand. This estimate of leaf area (L) is already corrected for the effect of leaf clumping at the crown level and stem area. The clumping of needles

Table 2
Means and standard errors in parentheses of estimates for Plot 1, a mixed-age stand at the old-growth ponderosa pine flux site

Variable	Plot 1
Live crown ratio (%)	53
Mean basal area (cm^2)	400 (48)
Annual foliage litter-fall biomass ($g\,m^{-2}$ ground)	174 (18)
Litter-fall SLA (cm^2 HSA g^{-1})[a]	43.8 (3.1)

[a] Specific leaf area (SLA) was calculate as half total surface area of needles of fresh litter (sampled on day 315).

within shoots (γ_E) and branch area index (B) were applied to obtain the final estimate of leaf area

$$L_{h3\text{-}D} = (L - B) \times \gamma_E \quad (7)$$

3. Results and discussion

3.1. Leaf area comparisons

Tables 2 and 3 show characteristics of Plot 1, and leaf area estimates obtained with various methods at this location. Comparison of the optical estimates from the LAI-2000 and the Ceptometer show that the L_{ecep} (1.7, S.E. = 0.2) was 30% greater than L_e calculated with LAI-2000 software (1.3, S.E. = 0.1),

Table 3
Leaf area estimated by the different methods for Plot 1 in 1997, where L_h is half-needle surface area per m^2 ground. S.E. in parentheses

Method	Plot 1	N
L_e[a]	1.3 (0.1)	242
L_{hc}[b]	1.7	
$L_{h3\text{-}D}$[c]	1.6 (0.01)	28000
L_{ecep}[d]	1.7 (0.2)	121
L_{hsw}[e]	3.7	593
L_{hlit}[f]	3.5	9

[a] Effective leaf area (L_e) from the LAI-2000 plant canopy analyzer measurements in 1997 and instrument software calculations (1-D model inversion).

[b] L_h from the LAI-2000, corrected for clumping and wood interception (Eq. (1)), where $\Omega_E = 0.81$ from the TRAC, $\gamma_E = 1.25$, $W = 0.27$.

[c] L_h from 3-D model, Eq. (7), where $\Omega_E = 0.83$ from the 3-D model, and $\gamma_E = 1.25$ from shoot measurements.

[d] L_e from Ceptometer measurements, Eq. (3).

[e] L_h from sapwood allometrics, Eq. (5).

[f] L_h from litter-fall estimates, Eq. (6).

where both methods assume a random distribution of foliage, which clearly is not the case in a semi-arid coniferous forest. Chen et al. (1997b) suggested that the Ceptometer estimates should be expected to be somewhat higher than the LAI-2000 L_e because the measurements account for the effect of foliage clumping at scales larger than the averaging length of the probe (80 cm), whereas the LAI-2000 L_e estimates ignore foliage clumping at all scales (both estimates include the effect of wood interception of light).

At Plot 1, we calculated the element clumping index, Ω_E, using several methods; Ω_E was 0.83 from the 3-D model, 0.75 from the tram measurements, and 0.81 from the TRAC measurements. Both the tram and 3-D model estimates were integrated over all solar zenith angles (θ) observed in summer, and the TRAC measurements were made at 34°. The lower value for the tram estimate could be partly explained by the small area sampled by the tram (36 m) and difficulties in gap removal decisions due to the frequent large gaps. The close comparison of the 3-D radiative transfer model estimate with the TRAC estimate is encouraging. Chen (1996) points out, however, that theoretically, the Ω_E should be determined over a range of θ, because Ω_E increases with θ between 30 and 80°, however, Chen and Cihlar (1995) found that inaccuracies in determining the small gaps only became serious when $\theta > 60°$. Because it was not logistically feasible to repeat TRAC measurements at a range of zenith angles at each plot in our study, we restricted measurement periods to $\theta = 25$–$50°$.

Wood area index, W, was 0.33 m^2 half-total wood area per m^2 ground for Plot 1 using the 3-D model estimate of S and our biomass estimate of half-branch area ($B = 0.10$), and W was 0.27 using our dimension estimates that account for stem taper.

When we used Eq. (1) to correct the LAI-2000 measurements (L_e 1.3 in 1997) for needle clumping within shoot ($\gamma_E = 1.25$, Law et al., 2001), clumping at scales larger than shoot (Ω_E from TRAC, 0.81), and wood area index ($W = 0.27$), L_{hc} was 1.7. When we used the 3-D model estimates of Ω_E and W, L_{hc} was still 1.7, and the $L_{h3\text{-}D}$ estimate from inversion of the 3-D model was 1.6 ((1.36–0.10) × 1.25, Eq. (5)).

The equations that we developed to estimate sapwood area from DBH are shown in Table 4. Estimates of leaf area for Plot 1 derived from sapwood and litter-fall were greater than the optical estimates

Table 4
Equations developed to convert from DBH to sapwood area for sapwood estimate of leaf area[a]

Plot	a	b	r^2	M.S.E.
1 (DBH <5 cm)	−0.1950	1.9828	0.96	0.0670
1 (DBH >5 cm)	0.0956	1.7406	0.78	0.1210
2	0.0956	1.7406	0.78	0.1210
3	−0.1950	1.9828	0.96	0.0670
4	0.2779	1.6337	0.98	0.1129
5	0.0940	1.8155	0.96	0.0367
6	−0.5540	2.2080	0.86	0.1775
7	−0.5540	2.2080	0.86	0.1775
8	−0.5540	2.2080	0.86	0.1775
9	−0.2480	2.0644	0.99	0.0327
10	−0.3160	2.1397	0.99	0.0123
11	−0.2263	2.0432	0.99	0.0231
15	0.7767	1.3905	0.86	0.1055
16	−0.2662	2.0695	0.99	0.0314
17	−0.1990	2.0174	0.99	0.0682
18	−0.6775	0.9687	0.95	0.0702
19	0.0940	1.8155	0.96	0.0367
20	0.1174	1.7155	0.87	0.0663

[a] $\log A_{sw} = a + b(\log \text{DBH})$.

(Table 3). L_h estimated from litter-fall was 3.5, which might be partly a result of scaling issues in determining plot mean SLA and foliage turnover rates. Estimates of L_h from litter-fall are influenced by the effect of the current climate on turnover rates, which must be characterized in the year of litter-fall collection (e.g. a drier than normal year can result in higher litter-fall rates).

The sapwood area estimate of L_h (L_{hsw}) for Plot 1 was 3.7, 54% higher than L_{hc}. When we evaluated the sapwood allometric approach for all 17 plots, in comparison with L_{hc}, the sapwood method resulted in leaf area values that were more than twice L_{hc} (Fig. 2, slope = 0.38). Sapwood area at only four of the plots was outside the range of values used to develop the allometric equation (Plots 1, 2, 4, 15). A commonly used ratio of sapwood to leaf area for ponderosa pine (0.19 LA:SA; Waring et al., 1982) was developed on small trees (maximum 150 cm^2/tree), and results in even larger estimates of L_{hsw}. Two primary concerns in selecting appropriate allometric equations are tree species and size. Studies have shown that estimating leaf area of trees with diameters that exceed the diameter range used for the allometric equation results in moderate to large overestimates of L_h (e.g. Gower et al., 1999). Differences in fertility and competition (stand density) will also affect estimates (Whitehead et al., 1984). For example, the ratio of sapwood area to DBH for 45-year-old pine trees in a heavily thinned stand nearby (Ryan et al., 2000) averaged 0.14, almost twice that of the same age trees in the mixed-age Plot 1 (0.08) where competition for resources is greater. At the thinned stand, the leaf area to sapwood area

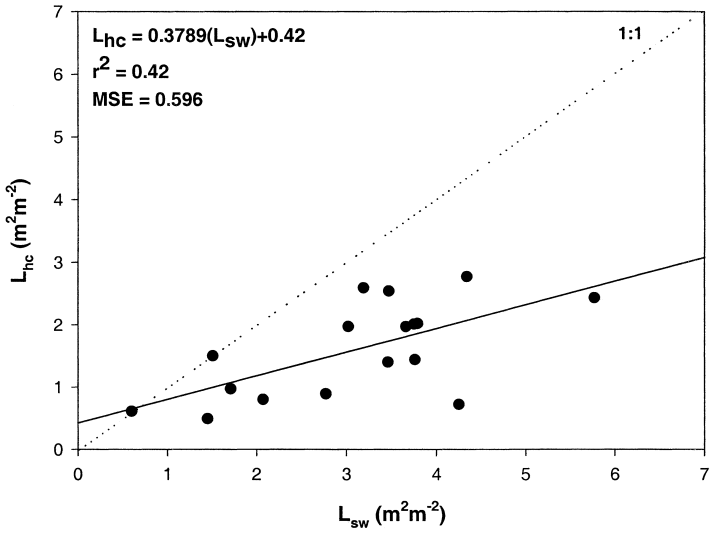

Fig. 2. Leaf area calculated from non-site-specific sapwood allometrics (L_{hsw}, m^2 half-surface area foliage per m^2 ground) tends to result in larger values of leaf area compared with LAI-2000 estimates corrected for clumping and wood interception (L_{hc}).

ratio for individual trees was lower for tall, old trees than young trees, LA:SA ($m^2\,cm^{-2}$) averaged 0.16 for 45-year-old trees, and 0.08 for 250-year-old trees. The highest LA:SA ratio for the 17 plots was 0.16 for Plot 15, matching that of the young trees in the Ryan et al. study. This plot was also heavily thinned, but it consisted of 64 and 158-year-old trees.

Sapwood to leaf area conversions are based on the pipe model theory that stems and branches are considered an assemblage of pipes that support a given amount of foliage (Shinozaki et al., 1964). Destructive harvest studies have shown the best correlation of leaf area with sapwood area were based on sapwood at the base of the live crown, and that sapwood area of ponderosa pines averaging 18 m in height decreased by 42% between DBH and the base of the crown (Waring et al., 1982).

Physiologically, the amount of foliage that can be supported by sapwood decreases as trees approach maximum height, likely because of hydraulic limitations to water transport in tall trees (Ryan et al., 2000). Whitehead et al. (1984) showed a linear relation between foliage area and the product of sapwood area and permeability across fertilized and control plots of *Picea sitchensis* and *Pinus contorta*, supporting the hypothesis that the relation between foliage area and sapwood area is dependent on permeability. They found that sapwood area, permeability and the product of these variables decreased with depth through the crowns of the trees. Thus, the assumption of constant permeability and sapwood fraction with height is invalid, so that the use of sapwood area at DBH to predict leaf area can lead to large overestimates. This would be particularly an issue in tall trees when allometrics are based on shorter trees. The approach may only be valid for short, young trees that are primarily sapwood.

It is generally suggested that non-optical estimates are more appropriate for stands with high leaf area, because optical measurements of L saturate at ~5–6 (Gower et al., 1999). The trade-off is that site-specific allometric equations for sapwood estimates are rare, permeability is not commonly measured, and repeat site visits through the year to collect litter-fall and fresh shoots for turnover rates, as well as scaling issues, limit the usefulness of these approaches over large areas.

Understory L_h estimated from three methods at Plot 20 was 0.13, 0.40, and 0.66 from destructive harvest of shrubs, the LAI-2000 method under individual shrubs, and LAI-2000 measurements at grid points (total L_e minus overstory L_e). Both of the optical methods include the effect of small trees, and the grid method likely accounts for more of the total understory because measurements under individual shrubs result in bias from the center ring (7°) capturing more of the shrub canopy.

3.2. Optical estimates of leaf area for all plots

We selected the 17 pine plots to obtain a range of stand densities and age classes in the 15 km swath (Table 1). The data from these plots in 1999 show that the TRAC estimates of Ω_E ranged from 0.49 to 1.00 for solar zenith angles 25–46° (Table 5; mean $\theta = 35°$, S.D. = 8). The solar zenith angle only explained about 13% of the variation in Ω_E across sites, partly because we attempted to make TRAC measurements in a restricted range of θ.

The Ω_E generally varies from 0.65 to 1.0, with higher values indicating less canopy clumping (Chen et al., 1997a). At the old-growth flux site, we observed less clumping in the dense 45-year-old stand (Plot 3, $\Omega_E = 0.86$), more clumping in the pure old-growth stand (Plot 2, $\Omega_E = 0.70$), and an intermediate value in the mixed-age stand ($\Omega_E = 0.81$), where θ was about the same during measurements at all three plots (33–34°).

The lowest Ω_E (0.49) was observed at Plot 15, which only had 34 trees/ha in the overstory (heavily thinned), and the highest value (1.00) was observed at an even aged 40-year-old stand (Plot 10) with a moderate stand density (395 trees/ha). The low Ω_E value for sparse vegetation (large gaps) appears to lead to erroneously high L_{hc} values; at Plot 15, the uncorrected L_e was 0.65, and L_{hc} was 1.5, yet the canopy was more sparse than the pure old-growth stand (Plot 2, $L_e = 0.66$, $L_{hc} = 0.9$). An even-aged, regularly spaced stand that had been thinned (Plot 9, 229 trees/ha) had Ω_E 0.84, similar to that of the mixed-age "natural" stand with a much higher density (Plot 1, $\Omega_E = 0.81$, 753 trees/ha), showing the interacting influence of stand density, vertical heterogeneity, and tree distribution on Ω_E. Stand density alone explained only 16% of the variation in Ω_E (Fig. 3).

L_{hc} ranged from 0.49 for a 52-year-old thinned stand (Plot 9, even aged, regularly spaced) to 2.77 for the

Table 5
Element clumping index (Ω_E), wood area index (W), and leaf area estimates for the ponderosa pine plots

Plot	Ω_E	W (m^2 HSA m^{-2})	L_e[a] (m^2 HSA m^{-2})	L_{hc}[b] (m^2 HSA m^{-2})	PAI[c] (m^2 HSA m^{-2})	L_{hc} total[d] (m^2 HSA m^{-2})	L_{hsw}[e] (m^2 HSA m^{-2})	Mean sapwood area/tree (cm^2)	Sapwood area (cm^2 m^{-2})	LA:Sa[f,g] (m^2 cm^{-2})
1	0.81	0.27	1.45	1.97	2.24	2.10	3.66	98.07, 2846.79	23.65	0.0832
2	0.70	0.29	0.66	0.89	1.18	1.02	2.77	2038.61	17.12	0.0521
3	0.86	0.46	1.99	2.43	2.89	2.53	5.77	291.35	37.47	0.0649
4	0.69	0.32	0.95	1.40	1.72	1.66	3.46	67.68, 3161.17	21.72	0.0642
5	0.62	0.26	1.11	1.97	2.23	2.40	3.02	501.69	19.16	0.1027
6	0.86	0.32	1.63	2.02	2.34	2.02	3.79	284.79	24.66	0.0821
7	0.55	0.39	1.50	2.77	3.16	3.22	4.34	538.63	27.43	0.1011
8	0.61	0.32	1.37	2.54	2.86	2.74	3.47	658.82	21.81	0.1163
9	0.84	0.17	0.45	0.49	0.66	0.89	1.45	440.49	9.25	0.0528
10	1.00	0.16	0.77	0.80	0.96	3.15	2.07	502.39	13.11	0.0609
11	0.73	0.27	1.33	2.01	2.27	2.06	3.75	649.62	23.57	0.0851
15	0.49	0.16	0.65	1.50	1.66	2.33	1.51	686.51, 3872.80	9.34	0.1608
16	0.95	0.30	1.32	1.44	1.74	1.95	3.76	519.79	23.83	0.0605
17	0.62	0.28	1.55	2.59	2.87	2.75	3.19	386.44	20.42	0.1269
18	0.74	0.33	0.75	0.72	1.05	1.46	4.25	576.50	26.79	0.0267
19	0.98	0.19	0.91	0.97	1.16	1.44	1.71	353.09	11.01	0.0877
20	0.97	0.01	0.13	0.61	0.62	1.01	0.60	44.63	5.77	0.1055

[a] Effective leaf area from LAI-2000 software.
[b] L_e corrected for clumping (Eq. (1)).
[c] Plant area index ($L_{hc} + W$).
[d] Total canopy L_{hc} (understory + overstory).
[e] L_h derived from sapwood area/DBH allometrics (Eq. (5)).
[f] Leaf area to sapwood area ratio (L_{hc} (m^2 m^{-2})/sapwood area (cm^2 m^{-2})).
[g] Leaf area to sapwood area ratio (L_{hc} (m^2 m^{-2})/sapwood area (m^2 m^{-2}).

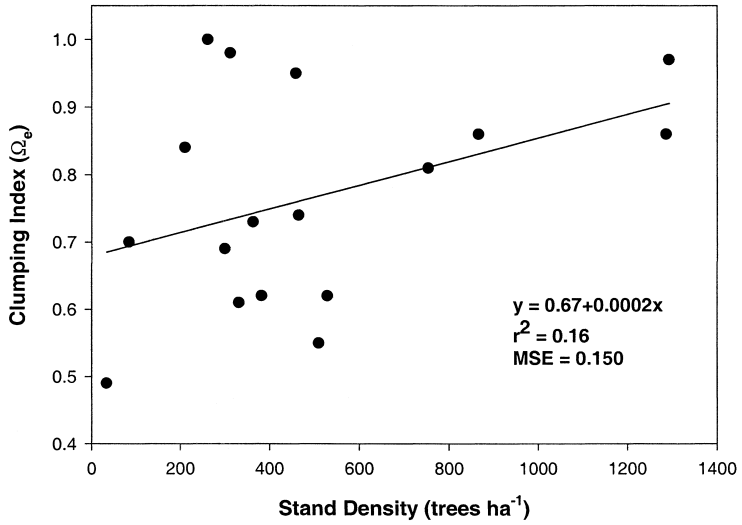

Fig. 3. Stand density explained 16% of the variation in clumping at scales larger than shoot (Ω_E) across the ponderosa pine plots.

97-year-old natural stand with moderate stand density (Plot 7). The probability density function for all plots centered on L_{hc} of 2 m^2 HSA m^{-2} ground (Fig. 4; S.D. = 0.57). L_{hc} at the flux sites appears to be representative of values for ponderosa pine in this region. L_{hc} for the old-growth flux site ranged from 0.9 in the pure old-growth stand to 2.4 in the 45-year-old stand (Plot 3), and 2.0 in the mixed-age stand (Plot 1; note this was observed in July 1999, and the 1.7 value for Plot 1 was observed in September 1997). At the 14-year-old pine flux site, L_{hc} was 0.6 for the trees, and 1.0 when shrubs were included in the estimate.

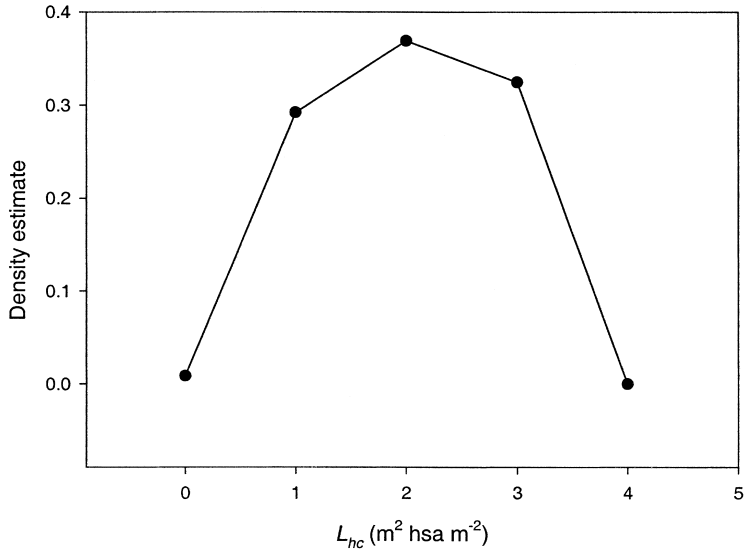

Fig. 4. The probability density function of leaf area (L_{hc}, m^2 HSA m^{-2}) for all plots, estimated from clumping-corrected LAI-2000 measurements, centered on 2 m^2 HSA m^{-2}.

In open forest canopies, it is critical to consider understory cover in validating ecosystem model estimates of leaf area and productivity. Natural regeneration with a minimum of management typically results in a large amount of understory cover, and in ponderosa pine forests, it often consists of nitrogen-fixing shrubs that can improve site fertility. On average, understory accounted for ~20% of the total L_{hc} (Table 5; mean understory $L_{hc} = 0.5$), and at plots with natural regeneration of young trees (Plots 10 and 20), the understory accounted for 35–60% of the total L_{hc}.

4. Conclusions

Common methods used to estimate LAI result in very different values for stands (Table 3), which particularly has implications to modeling ecosystem processes (Law et al., 2001). Sapwood allometric methods for estimating leaf area are commonly used for validation of models and remotely sensed data, yet this approach suffers from inaccuracies in allometry and scaling to the stand. Equations should be site-specific, accounting for influences of variation in wood permeability, site fertility, stand density, and tree size. The litter-fall method is not appropriate in coniferous forests because of climatic influences over the years of foliage retention, and scaling issues (SLA, turnover rates).

We favored an optical method, where the LAI-2000 data are corrected for clumping within shoot and scales larger than shoot in conifer forests, and interception of light by stems and branches. However, the calculation of Ω_E in sparse stands can lead to large overestimates of L_{hc}. The use of a TRAC instrument is relatively rapid, although we caution that it would be best to integrate estimates over a conservative range of solar zenith angles (e.g. 30–40°) because of diffuse sky conditions at large θ. The theoretical basis of using the LAI-2000 data, corrected for clumping, is sound, however, Eq. (1) might be modified in the future to account for integration of Ω_E over observed solar zenith angles, and to remove the effect of applying the within-shoot clumping factor to woody tissue.

For ponderosa pine forests in Central Oregon, we have often assumed a theoretical maximum LAI of 3 (lack of canopy closure), because of the dry climate. Our L_{hc} measurements showed a maximum of 2.8 for the overstory, or 3.2 total when understory was included in the estimate. At the stand level, leaf area appears to increase less at high sapwood areas, showing competition for resources in high density mature stands, and possible hydraulic limitations in sapwood that supports foliage in tall trees.

Acknowledgements

This study was funded by NASA (grant no. NAG5-8315 and no. NAG5-7551). We thank Sara Kerr, Greg Asner, and Robert Treuhaft for their contributions to field measurements, and Richard Waring for comments on an early draft of the manuscript. We gratefully acknowledge the assistance of Rod Bonacker at the Sisters Ranger District, and Sara Greene of the US Forest Service in establishing the flux site, which is located in a Research Natural Area — an area selected to represent vegetation types in a natural condition. We also thank Willamette Industries for allowing us access to their lands for this study, and our ongoing studies at the young pine flux site.

References

Baldocchi, D.D., Harley, P.C., 1995. Scaling carbon dioxide and water vapour exchange from leaf to canopy in a deciduous forest. II. Model testing and application. Plant Cell Environ. 18, 1157–1173.

Campbell, G.S., 1991. Application note: canopy LAI from Sunfleck Ceptometer PAR measurements. Decagon Devices, Inc., Pullman, WA.

Cescatti, A., 1997a. Modelling the radiative transfer in discontinuous canopies of asymmetric crowns. I. Model structure and algorithms. Ecol. Model. 101, 263–274.

Cescatti, A., 1997b. Modelling the radiative transfer in discontinuous canopies of asymmetric crowns. II. Model testing and application in a Norway spruce stand. Ecol. Model. 101, 275–284.

Chen, J.M., 1996. Optically-based methods for measuring seasonal variation of leaf area index in boreal conifer stands. Agric. For. Meteorol. 80, 135–163.

Chen, J.M., Black, T.A., 1992. Foliage area and architecture of plant canopies from sunfleck size distributions. Agric. For. Meteorol. 60, 249–266.

Chen, J.M., Blanken, P.D., Black, T.A., Guilbeault, M., Chen, S., 1997a. Radiation regime and canopy architecture in a boreal aspen forest. Agric. For. Meteorol. 86, 107–125.

Chen, J.M., Cihlar, J., 1995. Plant canopy gap-size analysis theory for improving optical measurements of leaf-area index. Appl. Opt. 34, 6211–6222.

Chen, J.M., Rich, P.M., Gower, S.T., Norman, J.M., Plummer, S., 1997b. Leaf area index of boreal forests: theory, techniques, and measurements, J. Geophys. Res. 102, 29, 429-29, 443.

Fassnacht, K.S., Gower, S.T., Norman, J.M., McMurtrie, R.E., 1994. A comparison of optical and direct methods for estimating foliage surface area index in forests. Agric. For. Meteorol. 71, 183–207.

Gholz, H.L., 1982. Environmental limits on aboveground net primary production, leaf area, and biomass in vegetation zones of the Pacific Northwest. Ecology 63, 469–481.

Gower, S.T., Norman, J.M., 1991. Rapid estimation of leaf area index in conifer and broad-leaf plantations. Ecology 72, 1896–1900.

Gower, S.T., Kucharik, C.J., Norman, J.M., 1999. Direct and indirect estimation of leaf area index, f_{APAR}, and net primary production of terrestrial ecosystems. Remote Sens. Environ. 70, 29–51.

Hollinger, D.Y., Goltz, S.M., Davidson, E.A., Lee, J.T., Tu, K., Valentine, H.T., 1999. Seasonal patterns and environmental control of carbon dioxide and water vapor exchange in an ecotonal boreal forest. Global Change Biol. 8, 891–902.

Houghton, R.A., Davidson, E.A., Woodwell, G.M., 1998. Missing sinks, feedbacks, and understanding the role of terrestrial ecosystems in the global carbon balance. Global Biogeochem. Cycles 12, 25–34.

Law, B.E., Cescatti, A., Baldocchi, D.D., 2001. Leaf area distribution and radiative transfer in open-canopy forests: implications to mass and energy exchange. Tree Physiol., 21.

Law, B.E., Waring, R.H., Anthoni, P.M., Aber, J.D., 2000a. Measurements of gross and net ecosystem productivity and water vapor exchange of a *Pinus ponderosa*ecosystem, and an evaluation of two generalized models. Global Change Biol. 6, 155–168.

Law, B.E., Williams, M., Anthoni, P.M., Baldocchi, D.D., Unsworth, M.H., 2000b. Measuring and modeling seasonal variation of carbon dioxide and water vapor exchange of a *Pinus ponderosa* forest subject to soil water deficit. Global Change Biol. 6, 613–630.

Law, B.E., Waring, R.H., 1994. Remote sensing of leaf area index and radiation intercepted by understory vegetation. Ecol. Appl. 4, 272–279.

Nilson, T., 1971. A theoretical analysis of the frequency of gaps in plant stands. Agric. Meteorol. 8, 25–38.

Norman, J.M., Jarvis, P.G., 1975. Photosynthesis in Sitka spruce (*Picea sitchensis*(Bong.) Carr.). V. Radiation penetration theory and a test case. J. Appl. Ecol. 12, 839–878.

Oechel, W.C., Vourlitis, G.I., Brooks, S., Crawford, T.L., Dumas, E., 1998. Intercomparison between chamber, tower, and aircraft net CO_2 exchange and energy fluxes measured during the Arctic Systems Science Land-Atmosphere-Ice-Interactions (ARCSS-LAII) flux study, J. Geophys. Res. 103, 28,993-29,003.

O'Hara, K.L., Valappil, N.I., 1995. Sapwood-leaf area prediction equations for mulit-aged ponderosa pine stands in wester Montana and Central Oregon. Can. J. For. Res. 25, 1553–1557.

Oker-Blom, P., Kellomaki, S., 1982. Effect of angular distribution of foliage on light absorption and photosynthesis in the plant canopy: theoretical computations. Agric. Meteorol. 26, 105–116.

Rosenberg, N.J., Blad, B.L., Verma, S.B., 1983. Microclimate and the Biological Environment, 2nd edition. John Wiley, New York, 495 pp.

Ryan, M.G., Bond, B.J., Law, B.E., Hubbard, R.M., Woodruff, D., Cienciala, E., Kucera, J., 2000. Transpiration and whole-tree conductance in ponderosa pine trees of different heights. Oecologia 124, 553–560.

Shinozaki, K., Yoda, K., Hozumi, K., Kira, T., 1964. A quantitative analysis of plant form-the pipe model theory. I. Basic studies. Jpn. J. Ecol. 14, 97–104.

Sprugel, D.G., 1983. Correction for bias in log-transformed allometric equations. Ecology 64, 209–210.

Stenberg, P., 1996. Correcting LAI-2000 estimates for the clumping of needles in shoots of conifers. Agric. For. Meteorol. 79, 1–8.

Turner, D.P., Cohen, W.B., Kennedy, R.E., Fassnacht, K.S., Briggs, J.M., 1999. Relationships between leaf area index and Landsat TM spectral vegetation indices across three temperate zone sites. Remote Sens. Environ. 70, 52–68.

VEMAP Members, 1995. Vegetation/ecosystem modeling and analysis project (VEMAP): comparing biogeography and biogeochemistry models in a continental-scale study of terrestrial ecosystem responses to climate change and CO_2 doubling. Global Biogeochem. Cycles 9, 407–437.

Waring, R.H., Schroeder, P.E., Oren, R., 1982. Application of the pipe model theory to predict canopy leaf area. Can. J. For. Res. 12, 556–560.

Whitehead, D., Edwards, W.R.N., Jarvis, P.G., 1984. Conducting sapwood area, foliage area, and permeability in mature trees of *Picea sitchensis* and *Pinus contorta*. Can. J. For. Res. 14, 940–947.